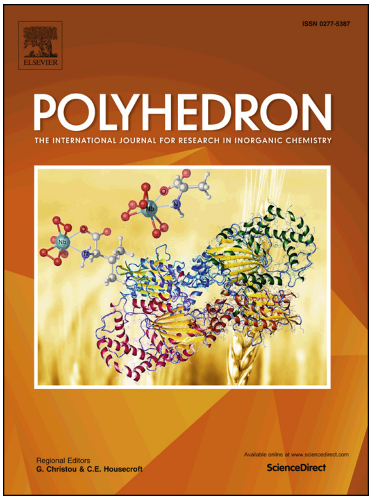

Experimental and theoretical studies on vanadium bromoperoxidase activity of alkyne arm dioxidovanadium(V) complex: crystal structure, spectral studies, and DFT calculations

M.A. Neelakantan, Chithiraivel Balakrishnan, P. Kowsalya, V. Selvarani

PII: S0277-5387(18)30076-7
DOI: https://doi.org/10.1016/j.poly.2018.02.009
Reference: POLY 13044

To appear in: *Polyhedron*

Received Date: 16 December 2017
Accepted Date: 9 February 2018

Please cite this article as: M.A. Neelakantan, C. Balakrishnan, P. Kowsalya, V. Selvarani, Experimental and theoretical studies on vanadium bromoperoxidase activity of alkyne arm dioxidovanadium(V) complex: crystal structure, spectral studies, and DFT calculations, *Polyhedron* (2018), doi: https://doi.org/10.1016/j.poly.2018.02.009

Experimental and theoretical studies on vanadium bromoperoxidase activity of alkyne arm dioxidovanadium(V) complex: crystal structure, spectral studies, and DFT calculations

M.A. Neelakantan*, Chithiraivel Balakrishnan, P. Kowsalya, V. Selvarani

Chemistry Research Centre, National Engineering College, K.R. Nagar, Kovilpatti - 628 503, Thoothukudi District, Tamil Nadu, India

*Corresponding Author
E-mail Address: drmaneelakantan@gmail.com

Abstract

The alkyne arm bearing dioxidovanadium(V) complex was synthesized by the reaction of vanadium sulphate, 1-[2-hydroxy-4-(prop-2-yn-1-yloxy)phenyl]ethanone and propane-1,2-diamine. The synthesized complex was characterized by various spectral techniques and its structure was determined using single-crystal X-ray diffraction analysis. Vanadium centre has square-pyramidal based geometry with an axial oxido ligand and the equatorial positions are occupied by another oxido ligand and phenolato oxygen, imine nitrogen and free amine nitrogen atoms. DFT and TD-DFT calculations were examined to identify the electronic structure, and electronic transitions of the complex observed in the absorption spectra. The percentage of intermolecular interactions in the crystal structure has been evaluated by 3D Hirshfeld surfaces and 2D fingerprint plots. The C-H···π and intermolecular interactions of the complex were examined using Bader's theory of QTAIM by ADF 2017. The dioxidovanadium(V) complex mimics as an efficient vanadium-dependent bromoperoxidase towards the bromination of phenol red in acetonitrile medium at room temperature.

Keywords: Dioxidovanadium(V) complex; Crystal structure; Non-covalent interactions; Bromoperoxidase activity

1. Introduction

Vanadium coordination chemistry has attracted increasing interest due to its presence in abiotic and biotic systems [1]. It is an ultra-trace element essential for healthy growth, development, and survival of higher organisms. The biological role of vanadium is evidenced from bacteria (vanadium replaces molybdenum in some azotobacter species) [2] and plants (in algae, lichens, and fungi as vanadium-dependent haloperoxidase) [3]. Vanadium exists in different oxidation states from -3 to +5 [4], and its coordination chemistry plays a vital role in the process of interaction with various biomolecules [5]. *In vivo*, under physiological conditions, vanadium complexes prevail in oxidation states +4 and +5. Vanadium is highly oxophilic in higher oxidation states [6]. In high-valant vanadium complexes, the element functions as an electron transfer catalyst in the processes of homolytic and heterolytic oxidation of organic substances [7] and have effects over biological systems [8]. The catalytic activity induces many researchers to develop innovative vanadium complexes mimicking vanadium-dependent haloperoxidase [9]. Recently, we reported the vanadium-dependent bromoperoxidase activity of some vanadium(IV) Schiff base complexes [10].

A wide range of weak intermolecular forces is involved in bio-molecular recognition processes, which helpfully demonstrate the binding attraction and specificity. Among the various intermolecular interactions [11], CH···π, H···H, and π··· π interactions attracted significant attention in recent years because of their importance in several areas of chemistry and biochemistry [12]. There are extensive explorations on non-covalent interactions in small organic molecules [13]. It is incredibly much essential to know the information of non-covalent interactions present in metal complexes, but the studies on these compounds are exceptionally scattered [14].

With all these in mind and continuation of our interest towards vanadium complexes, the present studies involve the synthesis of an alkyne arm bearing dioxidovanadium(V) complex and its structural analysis by spectral and single crystal X-ray techniques. The nature and percentage of intermolecular interactions in the crystal structure have been evaluated by 3D Hirshfeld surfaces and 2D fingerprint plots. The vanadium-dependent bromoperoxidase activity of the dioxidovanadium(V) complex was evaluated by the oxidative bromination of phenol red as a model substrate to bromophenol blue.

2. Experimental section

2.1. *Materials and physical methods*

2,4-dihydroxyacetophenone, propargyl bromide, potassium carbonate, and vanadyl sulphate was purchased from Sigma Aldrich and triethylamine from Merck. All the solvents were reagent grade and used as received. Elemental analyses were performed on a Thermo Finnigan Flash EA 1112 series carbon, hydrogen, and nitrogen analyzer. IR spectra were recorded on a Shimadzu 8400S spectrophotometer. Electronic absorption spectral measurement was carried out in acetonitrile using Shimadzu UV-2450 spectrophotometer.

2.2. *Synthesis of dioxidovanadium(V) complex*

A methanol solution (10 mL) of 1,2-diaminopropane (10 mM) was added to a methanolic solution of 1-[2-hydroxy-4-(prop-2-yn-1-yloxy)phenyl]ethanone (20 mM) and the resulting mixture was stirred and reflux for 2h. Then five mL aqueous solution of $VOSO_4$ (10 mM) was added followed by the addition of triethylamine (10 mM). The reaction mixture was refluxed for 3h. Filtration collected the yellow coloured precipitate and washed several times with hot ethanol and isopropyl alcohol (Scheme 1). The yellow crystals of suitable quality for X-ray analysis were obtained by slow evaporation of DMSO and methanol solution.

Yield: 89 %. Yellow color solid. M.P.: 245°C. Anal. Calcd. for $C_{14}H_{17}N_2O_4V$. Found (Calculated) (%) C: 51.22 (51.23), H: 5.20 (5.22), N: 8.52 (8.53). UV-Vis (CH_3CN): λ_{max} = 281, 332, 405 nm. FT-IR (KBr): ν, cm^{-1} 3271 (–C≡C–H), 2912 (asymmetric –C–H), 2845 (symmetric –C–H), 2116 (–C≡C–), 1601 (–C=N), 889, 915 (V=O). ^{51}V NMR (DMSO-d_6, ppm): –531.4.

2.3. *X-ray crystallography*

Single crystal X-ray data of dioxidovanadium(V) complex was collected using a Bruker Kappa Apex II X-ray diffractometer [15]. The X-ray radiation employed was generated from a Mo sealed X-ray tube ($K\alpha$ = 0.70173 Å at 296(2) K with a potential of 40 kV, 40 mA) connected with a graphite monochromator in the analogous mode. The relevant cell was finding out and refined by nonlinear least squares and Bravais lattice methods. The unit cell was established by checking the *h k l* overlays on different frames of data by comparing with both the orientation matrices. PARST and SHELXL-97 acquired the geometrical parameters. Hydrogen and non-hydrogen atoms were refined with anisotropic thermal parameters. Full matrix least square method on F^2 was refined to convergence the structure. Olex2 was utilized for the final data collection and structure plots [16].

2.4. Theoretical methods

The QTAIM analysis was performed by using the Amsterdam density functional (ADF) modeling suite (2017) [17] package at GGA:PW91 level and TZ2P basis set. QTAIM analysis provides topology properties such as electron density (ρ), Laplacian ($\nabla^2\rho$), local potential energy (V_b) and kinetic potential energy (G_b) at bond critical points for all the non-covalent contacts. The interaction energy for different intermolecular interactions was also calculated by using Espinosa-Molins-Lecomte (EML) relationship [18]. The molecular electrostatic potential analysis (MESP) has been performed using crystal explorer 3.1 software. Hirshfeld surface analysis and 2D fingerprint plots were also calculated using crystal explorer 3.1 [19a]. The molecular orbitals analysis [19b] and Mayer [19c] and orbital occupancy perturbed bond order [19d] calculations were done using the Multiwfn program [19e].

2.5. Vanadium bromoperoxidase activity

Bromination of phenol red to bromophenol blue utilizing dioxidovanadium(V) complex as a catalyst was studied by absorption spectroscopy. Bromination activity tests were done at a constant temperature of 30±0.5°C in the presence of H_2O_2 and KBr in the mild acidic medium. An aliquot of an acetonitrile solution of 0.1 mmol of catalyst was added to 30% H_2O_2 so that the final concentration of H_2O_2 in the reaction mixture was one mM, followed by the addition of $HClO_4$ (final concentration 2.0 mM) and 4.0 mol/L of KBr. Reactions were started by the addition of 0.25 mmol of phenol red, and the solution was stirred at a constant temperature of 25°C. The spectral measurements were kept at pH = 5.8 by the addition of NaH_2PO_4-Na_2HPO_4 [20]. The bromination reaction was observed by the slow vanishing of the ~400 nm band, and an increase in the absorbance of the peak at ~590 nm due to the development of the bromophenol blue product and spectral changes were recorded at the 5 min intervals. The reaction was complete under the ambient conditions after ∼4 h. The kinetic aspects of dioxidovanadium(V) complex were carried out by monitoring the increasing the formation of the product absorbance at ~590 nm by the initial rate method. The acetonitrile solution of 0.1 mmol of catalyst was added under stirring 0.1 mM 30% H_2O_2, 0.2 mM $HClO_4$ and 0.4 mmol of KBr and the reaction mixture was thermostated at 25°C.

With an increase of the substrate (phenol red) concentration from 10 to 50 equiv. with respect to the catalyst (0.1 mmol), the dependence of the rates on the substrate concentration was determined.

3. Results and discussion

3.1. Crystal structure description

The ORTEP diagram and atom numbering scheme of the dioxidovanadium(V) are shown in Fig. 1. The crystallographic data and structure refinement parameters, selected bond length and bond angles are presented in Tables 1 & 2. The asymmetric unit of the complex consists of monomeric dioxidovanadium(V) complex. The crystal structure of the compound crystallized into a centrosymmetric triclinic crystal system with P-1 space group. The vanadium atom of the complex is pentacoordinate in a square pyramidal environment coordinated to the tridentate Schiff base, via phenolic oxygen, N(amino-nitrogen) and N(azomethine) atoms and the remaining two coordinations are occupied by oxo groups. The geometry of penta-coordinated metal center is typically ascertained by the Addison parameter (τ) [$\tau = (\alpha-\beta)/60$, where α and β are the two major Ligand-Metal-Ligand angles of the coordination sphere (τ = ~0.00 for a square pyramid and τ = ~1.00 for a trigonal bipyramid)] [21a]. The calculated τ value of vanadium(V) complex is 0.042 indicates that the dioxidovanadium (V) complex have square pyramidal based geometry.

The crystal packing of dioxidovanadium(V) complex viewed down the '*a*' axis (Fig. S1) shows phenyl ring in planar conformation. The bond lengths of N(1)-V(1) and N(2)-V(1) are 2.1923(16) and 2.1113(16) Å, respectively. The bond length of O(1)-V(1), O(3)-V(1) and O(4)-V(1) are 1.899(13), 1.6160(15) and 1.6541(14) Å, respectively. The bond angles, O(3)-V(1)-O(4), O(3)-V(1)-O(1) and O(4)-V(1)-O(1) are 107.72(8)°, 103.90(7)° and 97.46(6)°, respectively. The bond angles of O(3)-V(1)-N(2) and O(4)-V(1)-N(2) are 96.63(7)° and 92.03(7)°, respectively. These bond length and bond angle values indicate that the present complex structure is square pyramid [21b]. The hydrogen bond parameters of the dioxidovanadium(V) complex are presented in Table 3. In dioxidovanadium(V) complex, the crystal packing is stabilized by N-H···O, C-H···O, and C-H···π intermolecular interactions. In the crystal structure, the molecules at (x, y, z) and (1-x, 1-y, 1-z;) are linked by C4-H4 ···O2 hydrogen bonds, generating a centrosymmetric dimeric ring motif $R_2^2(8)$ (Fig. 2). A weak intermolecular C10-H10···π interaction is also observed in the complex. The molecules at position (x,y,z) and (1+x,y,z) are linked by C-H···π interaction (Fig. 3), and so the H10 (bonded to C10) is at a distance of 2.81Å away from the centroid of the phenyl ring C2-C7(Cg^2) with C10 centroid distance of 3.615(3)Å. The propargyl group attached to the aromatic ring in the complex assumes an extended conformation, which can be seen from the O2-C8-C9-C10 torsion angles of -37(1)°. The C13 atom is found to be disordered over two sets of sites [site occupancies = 0.529(7) and 0.471(7)].

3.2. Spectroscopic studies

The IR spectrum of dioxidovanadium(V) complex shows several bands in the 400-4000 cm^{-1} region (Fig. S2). The compound 1-[2-hydroxy-4-(prop-2-yn-1-yloxy)phenyl]ethanone (A) exhibits a strong absorption band of carbonyl group frequency at 1631 cm^{-1}. This band disappears during the reaction of A with vanadium sulphate and propane-1,2-diamine, and a strong band at 1601 cm^{-1} corresponds to the presence of the azomethine -N coordinated to the vanadium ion [22]. The absorption at 3305 cm^{-1} corresponds to the N–H stretching frequency of complexed primary amino group. The C-O (phenolic) stretching appears at 1540 cm^{-1} in the complex indicates the coordination of deprotonated phenolic oxygen with the vanadium ion. The absorption band at 2912 cm^{-1} is due to the aromatic $\nu_{(C\text{-}H)}$ stretching of the complex. A medium absorption band at 2845 cm^{-1} indicates the presence of alkyl $\nu_{(C\text{-}H)}$ stretching. The complex exhibits medium absorption bands at 2116 cm^{-1} and at 1266 cm^{-1} corresponds to the presence of terminal alkyl group (-C≡C) and C-O-C (alkyl ether) stretching vibrations. The two vibrations at 889 and 915 cm^{-1} corresponds to the antisymmetric and symmetric stretching vibrations of the dioxidovanadium (V) moiety [21,23].

The electronic absorption spectrum of dioxidovanadium(V) complex was recorded in acetonitrile solution (Fig. S3a). The complex exhibits an intense band at 332 nm is assigned to $\pi(L) \rightarrow d_{\pi}(V)$ LMCT transition and another strong band at 405 nm is due to $\pi \rightarrow \pi^*$ transition of the ligand. The TD-DFT computed absorption spectrum of dioxidovanadium(V) complex is shown in Fig. S3b and the transitions are given in Table 5. The lowest energy absorption band at 417 nm is due to $\pi \rightarrow \pi^*$ transition of the ligand, whereas the strong absorption band appeared at 338 nm is due to the $\pi(L) \rightarrow d_{xz}(V)\text{-}p_x(O_{ax})$ LMCT transition of the metal complex. ^{51}V NMR spectrum of dioxidovanadium(V) complex was recorded in DMSO-d_6 solution (Fig. S4). The complex exhibits a single band at –531.4 ppm shows that the dioxidovanadium(V) complex occurs in the monomeric form [24].

The FMOs (Frontier Molecular Orbitals) of the dioxidovanadium(V) complex are given in Table 4 and Fig. S5. The orbital occupancy perturbed Mayer bond order calculations show that the LUMO is a weak antibonding orbital. The LUMO is mainly located in three metal-based orbitals such as $d_{xy}(V)$-$p_x(O_{eq})$ as LUMO+1, $d_{xz}(V)$-$p_x(O_{ax})$ as LUMO+3 and a d_{z}^{2} orbital as LUMO+2. These orbitals have an anti-bonding character for the V−O_{ax}, and V−O_{eq} interactions and the orbital percentage of vanadium metal ion is 68.7 % (LUMO+3), 70.3 % (LUMO+2) and 73.3 % (LUMO+1). These molecular orbitals reveal that covalent bonding is between the metal and ligand in dioxidovanadium(V) complex. Electron localization function (ELF) has been widely used for studying the nature of bond in organic and inorganic molecules, and the value is within the range of 0 to 1. The value of Mayer bond order is in agreement with the empirical bond order, for single, double and triple bond and the value is close to 1.0, 2.0 and 3.0 respectively. A large ELF value means that electrons are greatly localized, indicating that there is a covalent bond [19e]. The calculated electron localization function (ELF) values (η) for the dioxidovanadium(V) complex demonstrate that the V−O_{ax} and V−O_{eq} ($\eta = 0.94$ for V−O_{ax} and $\eta = 0.97$ for V−O_{eq}) bonds are strong in covalent bond character. The V−O1, V−N1 and V−N2 ($\eta = 0.72$ for V−O1, $\eta = 0.69$ for V−N1 and $\eta = 0.74$ for V−N2) bonds are weak in covalent bond character. The calculated Mayer bond orders (1.92 for V−O_{ax}, and 1.95 for V−O_{eq}, 0.63 for V−O1, 0.32 for V−N1 and 0.29 for V−N2, respectively) corroborate this [21b].

3.3. Hirshfeld surface analysis and 2D-Fingerprint plot

Hirshfeld surface and 2D fingerprint plot analysis were carried out to understand the various intermolecular interactions present in the dioxidovanadium(V) complex. Hirshfeld surface analysis shows that the structure of the complex is mainly characterized by H⋯H, O⋯H, and C–H⋯π contacts. The d_{norm} surfaces are mapped over a fixed color scale of -0.584 (red) to 1.193 Å (blue), shape-index mapped in the color range of -1.0 (concave) to 1.0 (convex) Å, and curvedness in the range of -4.0 (flat) to 4.0 (singular) Å (Fig. 4). In d_{norm} form, the color scale of red indicates shorter than van der Waals radii separation, white for equal van der Waals radii and blue indicates longer than van der Waals radii. These colors are used to visualize the intermolecular contacts. In d_{norm} form, the O⋯H interaction observed as the red areas (Fig. 4), and another spot in d_{norm} form corresponds to C⋯H and H⋯H interactions. The shape index indicates the shape of the electron density surface around the molecular interactions and the curvedness form shows the electron density around the molecule. The O⋯H intermolecular interactions appear as two distinct spikes of almost equal lengths in the 2D fingerprint plots. Among the two spike bottom left area (donor) corresponds to O⋯H interactions and bottom right (acceptor) corresponds to H⋯O interactions. Similarly, the C⋯H interactions also represented by a spike in the bottom left (donor) and H⋯C interactions posed by a spike in the bottom right (acceptor). The percentage of the intermolecular interactions are represented in Fig. 5. From the figure 4, the H⋯H contacts have the most significant contribution (38.2 %) to the total Hirshfeld surface, and is due to the presence of much higher propensity for H⋯H contacts. The contribution of O⋯H/H⋯O contacts in the complex is 30.4 %, and C⋯H/H⋯C is 26.1 % but this was overshadowed by the H⋯H contribution which is attributed due to the presence of $–CH_3$ substituent.

3.4. Molecular electrostatic potential(MSEP) maps

The MESP map is used to identify the electron rich and electron deficient sites of the complex and is useful in predicting the intermolecular interactions in the molecules (Fig. S6). In MESP maps, the positive electrostatic region/electron deficient /π-hole (blue region) indicates hydrogen donor potential whereas hydrogen bond acceptors are represented by negative electrostatic potential/electron rich/σ-hole (red region). The non-covalent interactions occur between the electropositive and electronegative regions. In dimer of the complex, the positive electrostatic region at hydrogen interacts with the negative electrostatic region at oxygen. Each benzene ring participates in two short C-H⋯π contacts interacting with the aliphatic hydrogen atoms. The chelate ring also interacts with aliphatic hydrogen and form C-H⋯π contacts.

3.5. QTAIM analysis

The strength of O⋯H/H⋯O, C⋯H/H⋯C interactions present in the dioxidovanadium(V) complex was studied by Bader’s theory of atoms in molecules (AIM). The AIM analysis for the dimer of the complex has been investigated by ADF using GGA:PW91 functional at TZ2P basis set [25]. It provides topological parameters including electron density and Laplacian operators at the bond critical points (Fig. 6 & Table S1). The Laplacian electron density values are positive indicates that closed-shell interactions are present in the dimer. The ratio of –|V|(r)/G((r) is less than unity suggests that all the interactions are non-covalent [26]. The local stabilization energy for the different non-covalent interactions was also estimated through an Espinosa-Molins-Lecomte (EML) relationship (I.E = 0.5 V_b, where V_b is local potential energy density at the BCP) [18]. Various intermolecular interactions stabilize the crystal packing. Among the interactions, C–H···π interactions having the higher interaction energy compared to that of O···H and chelating ring π-interactions. From these observations, it is clear that C–H···π interaction more stabilize the crystal packing. Similarly QTAIM analysis was studied for supramolecules of dioxidovanadium(V) complex. It also gave the same result which indicates that all the interactions are non-covalent in nature and C–H···π interaction stabilizes crystal packing (Fig. S7 & Table S1).

3.6. Vanadium haloperoxidases activity

Vanadium haloperoxidase (VHPO) catalyzes the bromination of organic compounds in the presence of hydrogen peroxide (H_2O_2) and potassium bromide (KBr). Metal complexes, which are capable of catalyzing bromide oxidation are considered as functional bromoperoxidase mimics [27]. The bromoperoxidase activity of the metal complexes has been measured by the kinetic study of catalytic bromination of phenol red to bromophenol blue [28]. The catalytic activity of synthesized dioxidovanadium(V) complex was examined using phenol red as a model organic substrate, which is converted to bromophenol blue during the reaction (Scheme S1) and the course of the reaction was monitored using electronic absorption spectroscopy. The addition of dioxidovanadium(V) complex to the substrate gradually decreases the absorption intensity of phenol red at 443 nm, and a new band appears at 592 nm due to bromophenol blue. This demonstrates that the dioxidovanadium(V) complex acts as a catalyst for the conversion of phenol red to bromophenol. The formation of the isosbestic point at 490 nm support the catalytic conversion phenol red to bromophenol blue (Fig. 7a). The Michaelis-Menten model developed for enzyme kinetics was used to study the kinetics of oxidation of bromophenol in the presence of dioxidovanadium(V) complex as a catalyst, exhibit saturation kinetics (Fig. 7b). Hanes-Woolf plot of [S]/rate vs. [S] was used to calculate the Michaelis-Menten binding constant (K_M), maximum velocity (V_{max}) and rate constant for dissociation of substrates (k_{cat}) (Fig. 7c & Table 5). An experiment conducted in the absence of dioxidovanadium(V) complex shows no change in the absorbance at 495 nm demonstrate the effect of dioxidovanadium(V) complex as catalyst (Fig. 7d). The probable mechanism of the catalytic process under the mild acidic condition is the dioxidovanadium(V) (A) which acts as a catalyst is first converted into hydroxyl intermediate (B). In the presence of H_2O_2, the hydroxyl species leads to transient formation peroxido intermediates (C-E) and finally dioxiran-1-ium ion intermediate (F). The dioxiran-1-ium ion intermediate (F) oxidizes the bromide ion (Br^-) into bromonium ion intermediate (G). The intermediate G accept a proton from a surrounding water molecule leads to the formation of hypobromite adduct (H) with the release of hypobromous acid (HOBr) followed by renovation of the native state (A) [29]. The TD-DFT computational study was employed to support the experimental investigations of catalytic conversion of phenol red to bromophenol blue in the presence of dioxidovanadium(V) complex as catalyst (Fig. S8). The UV-vis spectra were computed for transiently formed intermediate species (B-F). The observed results show that peroxo species formation is accompanied by the disappearance of the intense band at 331 nm is in good agreement with the experimental data.

4. Conclusions

Dioxidovanadium(V) complex has been synthesized and characterized by different spectral techniques. Single crystal X-ray diffractcion analysis has structurally characterized the structure of the complisex reveal square pyramidal based geometry around the vanadium ion. The intermolecular interactions present in the complex studied by Hirshfeld surface analysis shows that the structure of the complex is mainly characterized by H⋯H, O⋯H, and C–H⋯π contacts, with the H⋯H contacts, have 38.2% contribution to the total Hirshfeld surface. The QTAIM studies suggest that C–H⋯π interaction more stabilize the crystal packing. The synthesized compound exhibit bromoperoxidase activity by converting the model substrate, phenol red to bromophenol blue, efficiently mimicking the functional models of vanadium-dependent bromoperoxidase enzyme.

Acknowledgement

Dr. M.A.N. gratefully acknowledged the financial support from Science and Engineering Research Board (SERB), Department of Science and Technology (DST), Government of India, New Delhi (EMR-II/2014/000081). C. B is thankful to CSIR, India for his fellowship. STIC, Cochin is acknowledged for performing the SCXRD analysis.

Supplementary data

CCDC 882668 contains the supplementary crystallographic data for dioxidovanadium(V). The data can be obtained free of charge via http://www.ccdc.cam.ac.uk/conts/retrieving.html or from the Cambridge Crystallographic Data Centre, 12 Union Road, Cambridge CB2 1EZ, UK; fax: (+44) 1223-336-033; or e-mail: deposit@ccdc.cam.ac.uk.

References

[1] a) P. Frank, R.M.K. Carlson, E.J. Carlson, K.O. Hodgson, Coord. Chem. Rev. 237 (2003) 31; b) R.E. Berry, E.M. Armstrong, R.L. Beddoes, D. Collison, S.N. Ertok, Helliwell, C.D. Mand, Garner, Angew. Chem., Int. Ed. 38 (1999) 795; c) D. Rehder, Angew. Chem., Int. Ed. Engl. 30 (1991) 148.

[2] A. Butler, J.V. Walker, Chem. Rev. 93 (1993) 1937.

[3] a) R. Wever, B. E Krenn, N. D. Chasteen, Ed., Kluwer Academic Publishers, Dordrecht, 1990, 81; b) M.G. Almeida, M. Humanes, R. Melo, J.A. Silva, J.J.R.F. da Silva, R. Wever, Phytochemistry 54 (2000) 5.

[4] G. Wilkinson, (Ed.), Comprehensive Coordination Chemistry, Pergamon Press, Oxford (1987).

[5] E.C. Theil, K.N. Raymond, I. Bertini, H.B. Gray, S.J. Lippard, J.S. Valentine, University Science Books, Mill Valley, CA (1994) 1.

[6] N.D. Chasteen, Vanadium in Biological Systems: Physiology and Biochemistry, Kluwer Academic Dordrecht (1990).

[7] a) V. Conte, A. Coletti, B. Floris, G. Licini, C. Zonta, Coord. Chem. Rev. 255 (2011) 2165; b) G. Romanowski, J. Mol. Catal. A: Chem. 368 (2013) 137.

[8] F. Montilla, D. del Rio, A. Pastor, A. Galindo, Organomet. 25 (2006) 4996.

[9] a) R.I. de la Rosa, M.J. Clague, A. Butler, J. Am. Chem. Soc. 114 (1992) 760; b) L.J. Calviou, D. Collison, C.D. Garner, F.E. Mabbs, M.A. Passand, M. Pearson, Polyhedron 8 (1989) 1835.

[10] a) M.A. Neelakantan, C. Balakrishnan, V. Selvarani, M. Theetharappan, Appl. Organomet. Chem. (2017) e4125; b) C. Balakrishnan, M.A. Neelakantan, Inorg. Chim. Acta 469 (2018) 503.

[11] a) C.A. Hunter, J.K.M. Sanders, J. Am. Chem. Soc. 112 (1990) 5525; b) C. Caltagirone, P.A. Gale, Chem. Soc. Rev. 38 (2009) 520; c) A. Frontera, P. Gamez, M. Mascal, T.J. Mooibroek, J. Reedijk, Angew. Chem. Int. Ed. 50 (2011) 9564; d) A. Frontera, Coord. Chem. Rev. 257 (2013) 1716; e) A. Bauza, T.J. Mooibroek, A. Frontera, Angew. Chem., Int. Ed. 52 (2013) 12317; f) M.M. Watt, M.S. Collins, D.W. Johnson, Acc. Chem. Res. 46 (2013) 955.

[12] a) S.S. Tandon, S.D. Bunge, N. Patel, J. Sanchiz, Polyhedron 123 (2017) 361; b) A.M. Beatty, Coord. Chem. Rev. 246 (2003) 131; c) C. Rest, M.J. Mayoral, K. Fucke, J. Schellheimer, V. Stepanenko, G. Fernandez, Angew. Chem. Int. Ed. 53 (2014) 700; d) A.D. Brathwaite, T.B. Ward, R.S. Walters, M.A. Duncan, J. Phys. Chem. A 119 (2015) 5658; d) P. Bhowmik, S. Chatterjee, S. Chattopadhyay, Polyhedron 63 (2013) 214; e) S. Canellasa, A. Bauza, A. Lancho, A.G. Raso, J.J. Fiol, E. Molins, P. Ballester, A Frontera, Cryst. Eng. Comm. 17 (2015) 5987.

[13] a) G.R. Desiraju, Chem. Commun. (1997) 1475; b) G.R. Desiraju, J. Chem. Sci. 122 (2010) 667.

[14] a) A. Tasada, F.M. Alberti, A. Bauza, M.B. Oliver, A.G. Raso, J.J. Fiol, E. Molins, A. Caubet, A. Frontera, Chem. Commun. 49 (2013) 4944; b) M. Mitra, P. Manna, S.K. Seth, A. Das, J. Meredith, M. Helliwell, A. Bauza, S. Ray Choudhury, A. Frontera, S. Mukhopadhyay, Cryst Eng. Comm. 15 (2013) 686.

[15] APEX2 “Program for Data Collection on Area Detectors” BRUKER AXS Inc., 5465 East Cheryl Parkway, Madison, WI 53711-5373, USA.

[16] O.V. Dolomanov, L.J. Bourhis, R.J. Gildea, J.A.K. Howard, H. Puschmann, J. Appl. Cryst. 42 (2009) 339.

[17] a) C.F. Guerra, F.M. Bickelhaupt and E. J. Baerends, Cryst. Growth Des. 2 (2002) 239; b) R.F.W. Bader, Atoms in molecules, A quantum theory, Oxford University Press, Oxford (1990).

[18] E. Espinosa, E. Molins, C. Lecomte, Chem. Phys. Lett. 285 (1998) 170.

[19] a) S.K. Wolff, D.J. Grimwood, J.J. McKinnon, M.J. Turner, D. Jayatilaka, M. Spackman, Crystal Explorer, version 3.1, Revision, University of Western Australia, Crawley (2012) 1448; b) R.S.J. Mulliken, Chem. Phys. 23 (1955) 1833; c) I. Mayer, Theor. Chim. Acta 67 (1985) 315; d) S.I.J. Gorelsky, Chem. Theory Comput. 8 (2012) 908; e) T. Lu, F. Chen, J. Comput. Chem. 33 (2012) 580.

[20] E. Verhaeghe, D. Buisson, E. Zekri, C. Leblanc, P. Potin, Y. Ambroise, Anal. Biochem. 379 (2008) 60.

[21] a) A.W. Addison, T.N. Rao, J. Reedijk, J. van Rijn, G.C. Verschoor, J. Chem. Soc. Dalton Trans. (1984) 1349; b) C. Das, P. Adak, S. Mondal, R. Sekiya, R. Kuroda, S.I. Gorelsky, S.K. Chattopadhyay, Inorg. Chem. 53 (2014) 11426;.

[22] a) G.C. Percy, D.A. Thornton, J. Inorg. Nucl. Chem. 34 (1972) 3369; b) G. Kolawole, K.S. Patel, J. Chem. Soc., Dalton Trans. (1981) 1241.

[23] G. Asgedom, A. Sreedhara, J. Kivikoski, J. Valkonen, C.P. Rao, J. Chem. Soc., Dalton Trans. (1995) 2459.

[24] a) E. Kwiatkowski, G. Romanowski, W. Nowicki, M. Kwiatkowski, K. Suwinska, Polyhedron 22 (2003) 1009; b) E. Kwiatkowski, G. Romanowski, W. Nowicki, M. Kwiatkowski, K. Suwinska, Polyhedron 26 (2007) 2559; c) G. Romanowski, E. Kwiatkowski, W. Nowicki, M. Kwiatkowski, T. Lis, Polyhedron 27 (2008) 1601; d) C.A. Root, J.D. Hoeschele, C.R. Cornman, J.W. Kampf, V.L. Pecoraro, Inorg. Chem. 32 (1993) 3855.

[25] S. Gandhimathi, M. Theetharappan, N.S.P. Bhuvanesh, M.A. Neelakantan, Polyhedron 138 (2017) 88.

[26] a) B.M. Draskovic, G.A. Bogdanovic, M.A. Neelakantan, A.C. Chamayou, S. Thalamuthu, Y.S. Avadhut, J.S. Gunne, S. Banerjee, C. Janiak, Cryst. Growth Des. 10 (2010) 1665; b) J. Paredes, R.C.C. Torres, O.H. Negrete, R.R.S. Mundo, D.G. Mitnik, H.E.E. Ponce, M.E.A. Ramos, J. Mol. Struct. 1141 (2017) 53.

[27] P. Adak, B. Ghosh, B. Pakhira, R. Sekiya, R. Kuroda, S.K. Chattopadhyay, Polyhedron 127 (2017) 135.

[28] a) S.L. Neidleman, J.L. Geigert, Biohalogenation, Ellis Horwood Ltd. Press, New York, 1986; b) G.J. Colpas, B.J. Hamstra, J.W. Kampf, V.L. Pecoraro, J. Am. Chem. Soc. 118 (1996) 3469; c) G.J. Colpas, B.J. Hamstra, J.W. Kampf, V.L. Pecoraro, J. Am. Chem. Soc. 116 (1994) 3627.

[29] a) G. Zampella, P. Fantucci, V.L. Pecoraro, L.D. Gioia, J. Am. Chem. Soc. 127 (2005) 953; b) J.Y. Kravitz, V.L. Pecoraro, H.A. Carlson, J. Chem. Theory Comput. 1 (2005) 1265; c) G. Zampella, P. Fantucci, V.L. Pecoraro, L.D. Gioia, Inorg. Chem. 45 (2006) 7133.

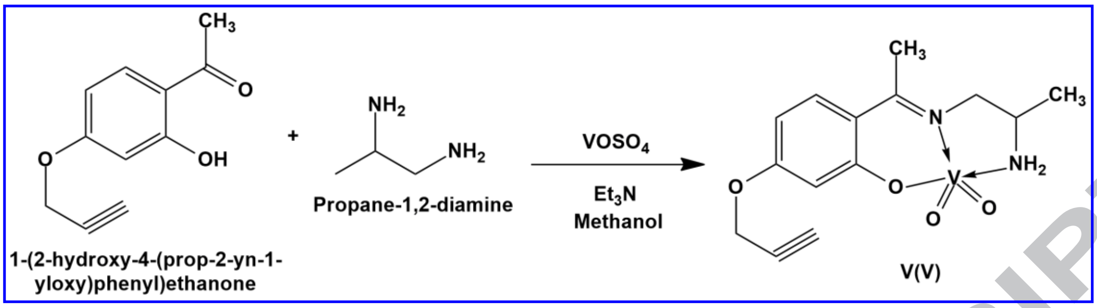

Scheme 1 Synthesis of dioxidovanadium(V) complex

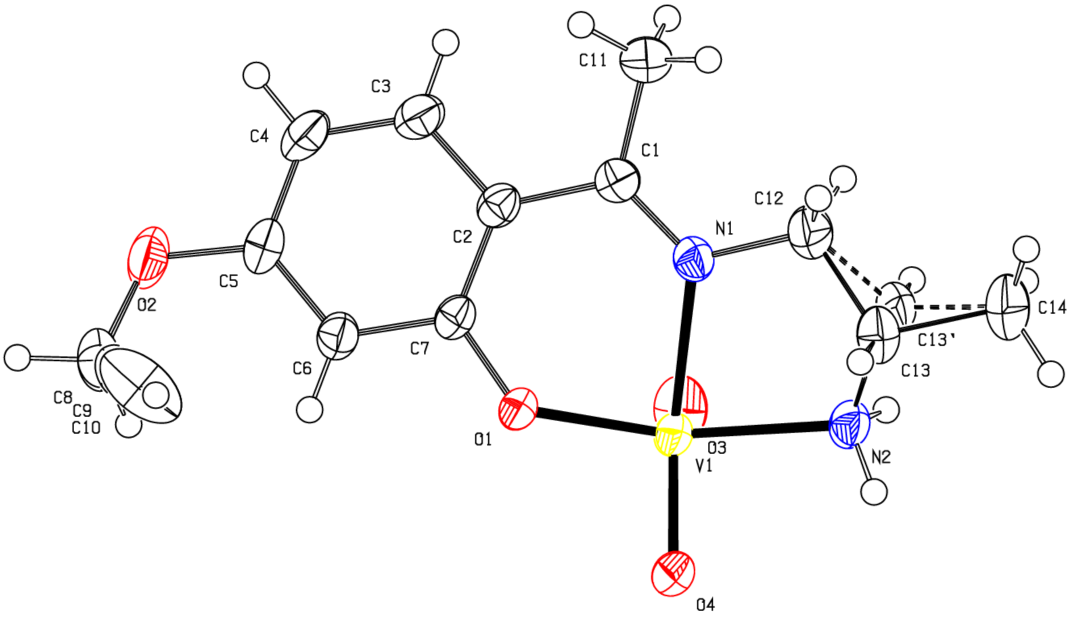

Fig. 1. ORTEP view (50% probability level) of the molecular structure of dioxidovanadium(V) complex.

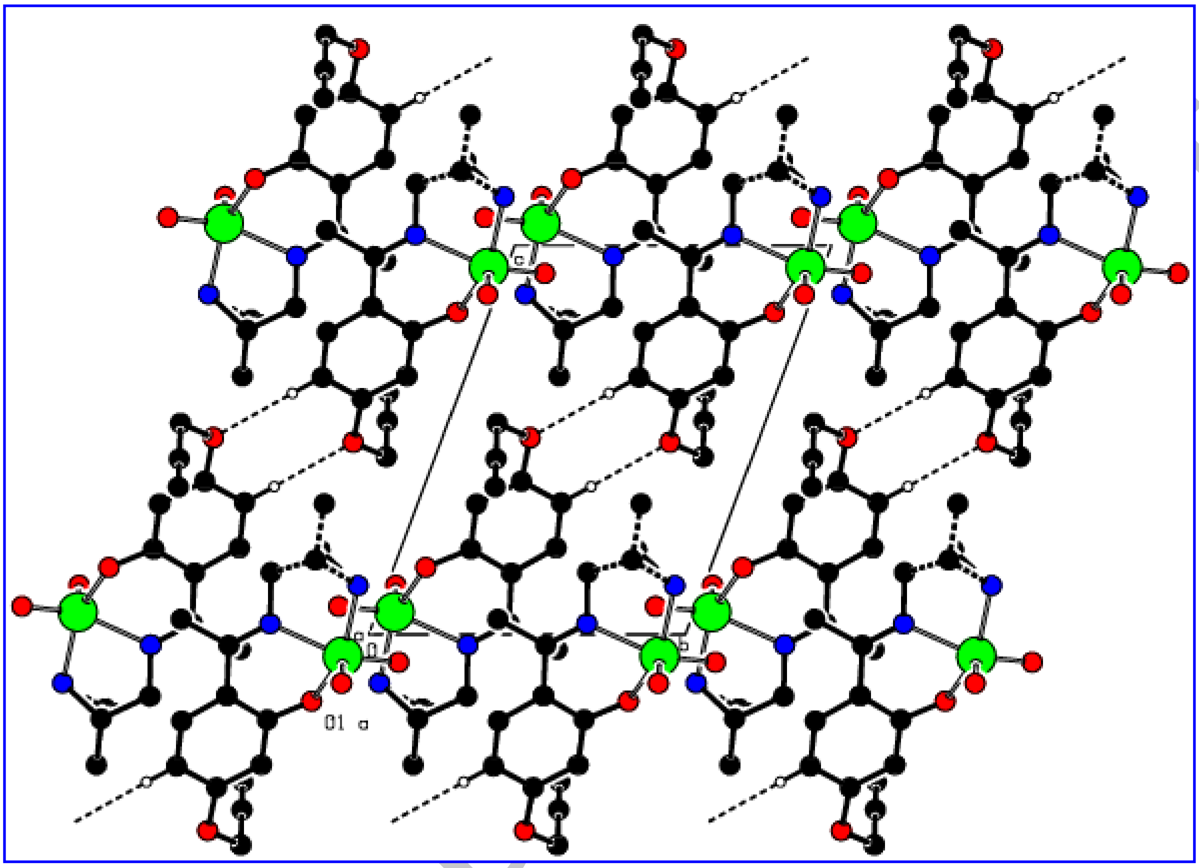

Fig. 2. Crystal packing diagram of dioxidovanadium(V) complex, showing the formation of centrosymmetric $R_2^2(8)$ dimer.

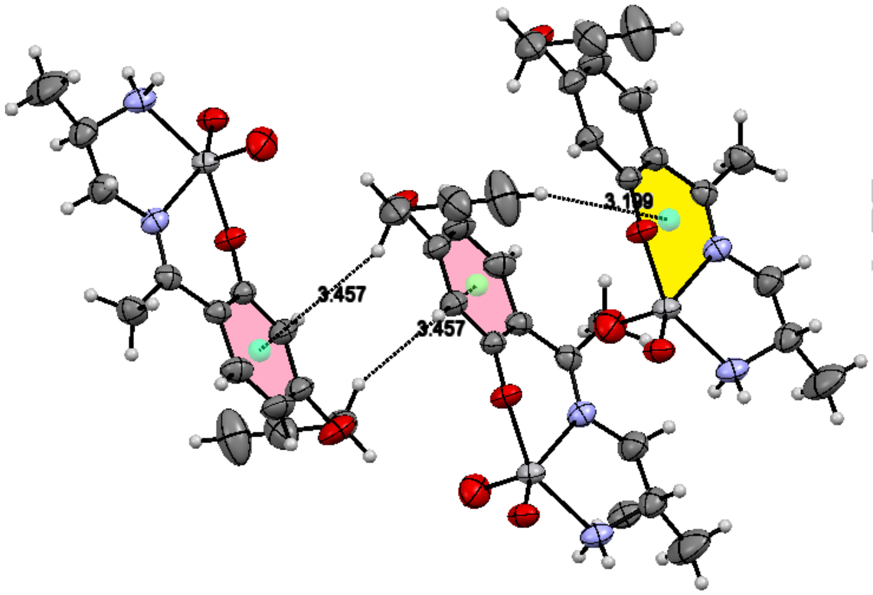

Fig. 3. C-H···π interaction for the dioxidovanadium(V) complex.

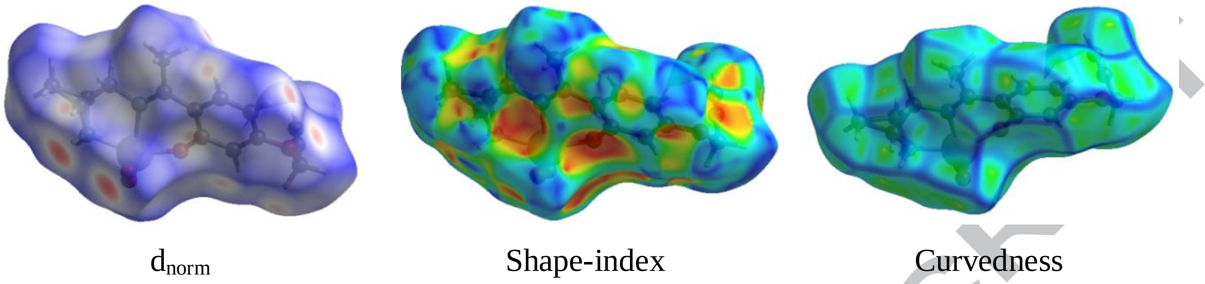

Fig. 4. Hirshfeld surfaces mapped over d_{norm}, shape index, d_i and d_e form of dioxidovanadium(V) complex.

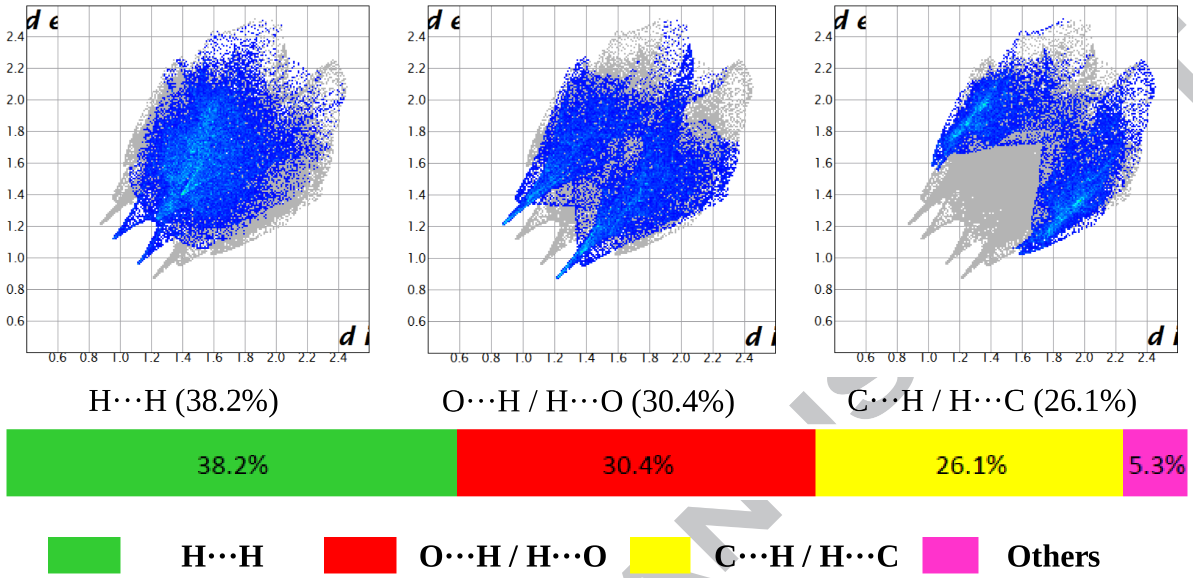

Fig. 5. 2D Fingerprint plots of dioxidovanadium(V) complex, H···H (left), O···H/H···O (middle) and C···H/H···C (right) contacts showing the percentage of contact contributed to the total Hirshfeld surface area of the molecule.

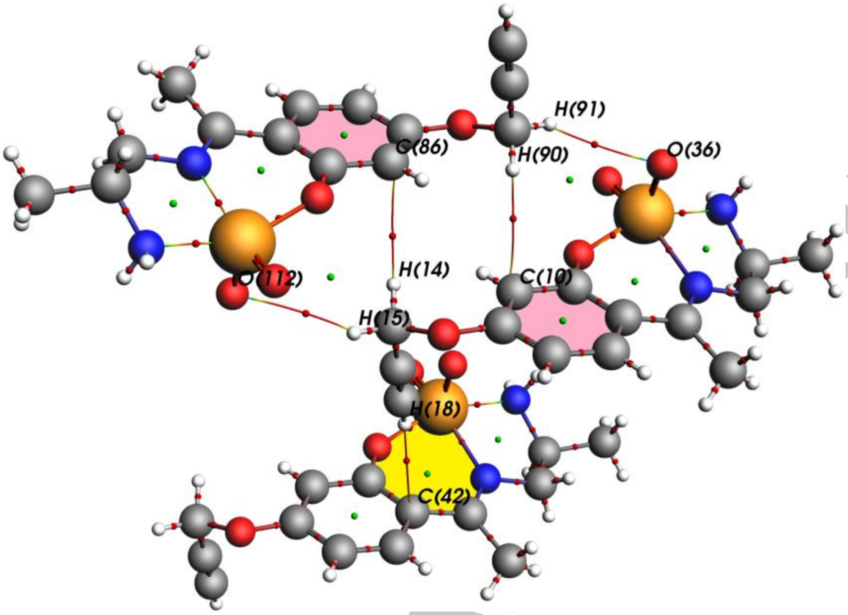

Fig. 6. Molecular plots for dimers dioxidovanadium(V) complex showing the different intermolecular contacts in the presence of bond critical points (red spheres).

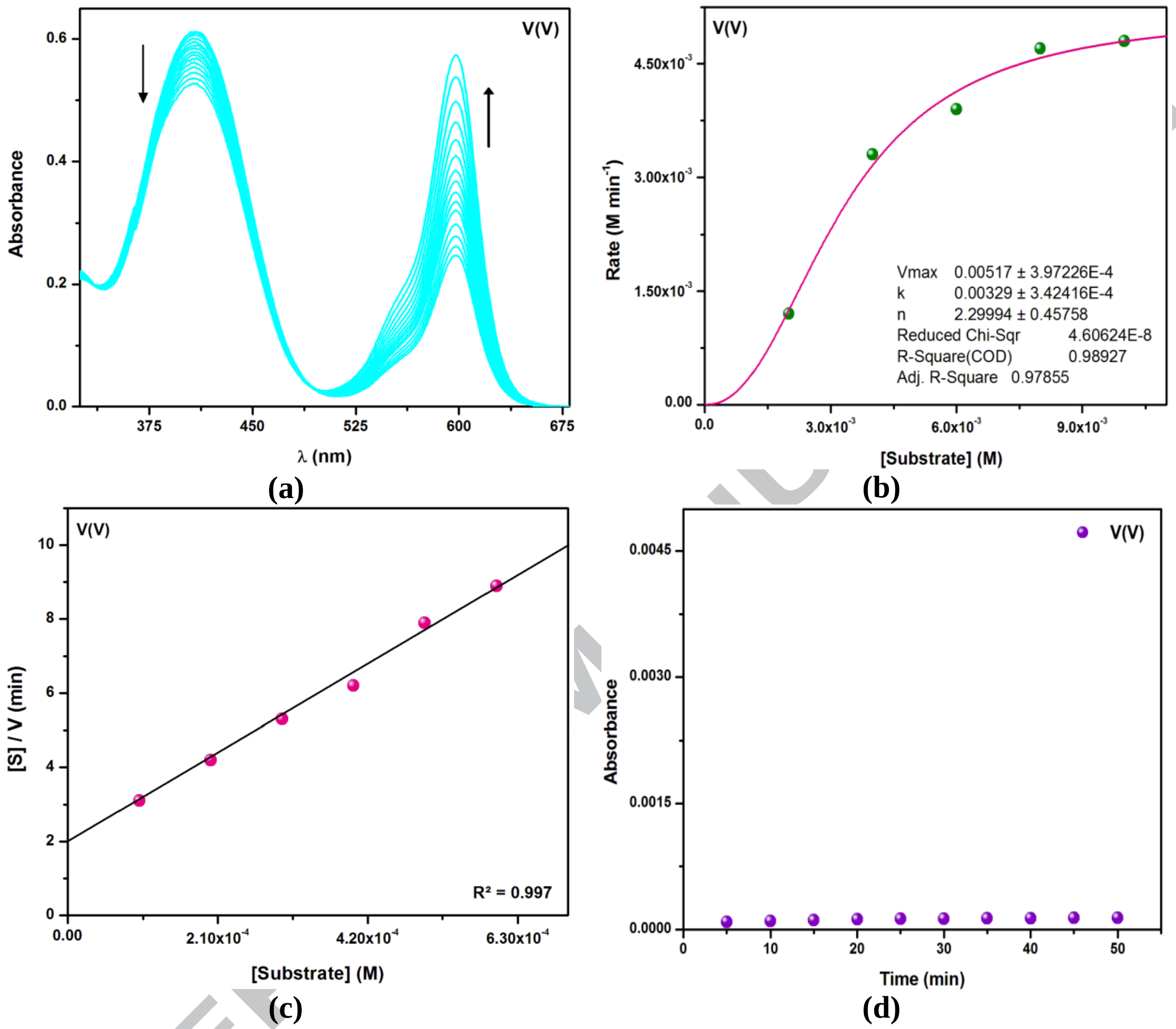

(a) (b)

(c) (d)

Fig. 7. (a) Oxidative bromination of phenol red (1.0×10^{-3} M) catalyzed by dioxidovanadium(V) complex (10^{-4} M) in acetonitrile; (b) Plot of rate vs. substrate concentration for dioxidovanadium(V) complex; (c) Hanes-Woolf plot for dioxidovanadium(V) complex and (d) Absorbance vs. Time plot of a mixture of KBr, H_2O_2, $HClO_4$ and Phenol red in absence of dioxidovanadium(V) complex.

Table 1

Crystallographic data and collection parameters for dioxidovanadium(V) complex.

Parameters	dioxidovanadium(V) complex
Empirical formula	$C_{14}H_{17}N_2O_4V$
Formula weight	328.24
Temperature	293(2) K
Wavelength	0.71073 A
Crystal system, space group	Triclinic, *P*-1
Unit cell dimensions	
a = 7.6670(9) (Å)	α = 69.383(7) (˚)
b = 8.7413(11) (Å)	β = 88.086(5) (˚)
c = 11.3835(14) (Å)	γ = 83.115(5) (˚)
Volume	708.88(15) (Å^3)
Z, Calculated density	2, 1.538 Mg/m^3
Absorption coefficient	0.717 mm^{-1}
F(000)	340
Crystal size(mm)	0.24 × 0.21 × 0.2
Theta range for data collection	1.91 to 28.35 (˚)
Limiting indices	-10<=h<=10, -11<=k<=11, -14<=l<=15
Reflections collected / unique	12703 / 3510 [R(int) = 0.0240]
Refinement method	Full-matrix least-squares on F^2
Data / restraints / parameters	2510 / 3 / 210
Goodness-of-fit on F^2	1.048
Final R indices [I>2σ(I)]	R1 = 0.0357, wR2 = 0.0966
R indices (all data)	R1 = 0.0425, wR2 = 0.1016
Largest diff. peak and hole	0.559 and -0.417 (e. Å^{-3})

Table 2

Selected bond lengths (Å) and bond angles (°) for dioxidovanadium(V) complex.

Bond length (Å)		Bond angle (°)	
C(1)-N(1)	1.290(2)	O(3)-V(1)-O(4)	107.72(8)
N(1)-V(1)	2.1923(16)	O(3)-V(1)-O(1)	99.95(7)
N(2)-V(1)	2.1113(16)	O(4)-V(1)-O(1)	97.46(6)
O(1)-V(1)	1.8993(13)	O(3)-V(1)-N(2)	96.63(7)
O(3)-V(1)	1.6160(15)	O(4)-V(1)-N(2)	92.03(7)
O(4)-V(1)	1.6541(14)	O(1)-V(1)-N(2)	153.46(6)
C(7)-O(1)	1.319(2)	O(3)-V(1)-N(1)	96.87(8)
C(9)-C(10)	1.160(4)	O(4)-V(1)-N(1)	154.31(7)
C(10)-H(10)	0.9300	O(1)-V(1)-N(1)	83.39(6)
C(1)-C(11)	1.511(3)	N(2)-V(1)-N(1)	77.55(6)
C(11)-H11(A)	0.9600	N(2)-C(13)-H(13)	109.5
C(11)-H11(B)	0.9600	C(14)-C(13)-H(13)	109.5
C(11)-H11(C)	0.9600	C(12)-C(13')-N(2)	108.9(2)
C(13)-N(2)	1.493(3)	O(3)-V(1)-O(4) #1	172.23(7)
C(12)-N(1)	1.469(3)	O(4)-V(1)-O(4) #1	77.86(6)
C(13)-C(14)	1.561(3)	O(1)-V(1)-O(4) #1	80.32(5)
C(12)-C(13)	1.482(4)	N(2)-V(1)-O(4) #1	77.53(5)
O(4)-V(1)#1	2.4603(15)	N(1)-V(1)-O(4) #1	79.98(5)

Table 3

Hydrogen bonding parameters for dioxidovanadium(V) complex, D = donor, A = acceptor (Å, °).

D–H···A	D–H	H···A	D···A	D–H···A
N2-H2A···O1$^{(i)}$	0.90	2.18	2.940(2)	141
N(2)-H(2B)···O(3)$^{(ii)}$	0.90	0.90	3.033(2)	158
C4-H4···O2$^{(iii)}$	0.93	2.54	3.446(3)	166
C11-H11B···O4$^{(iv)}$	0.96	2.52	3.472(3)	170
C10-H10···Cg2$^{(v)}$	-	2.81	3.614(3)	145

Symmetry codes: (i) 1-x,-y,-z; (ii) -x,-y,-z (iii) 1-x,1-y,1-z; (iv) x,1+y,z ; (v) 1+x,y,z and Cg^2 is the centroid of the C2-C7 ring.

Table 4

Energies and Mulliken population analysis derived FMO compositions of dioxidovanadium(V) complex

Molecular orbital	Description	Contribution (%)				
		L	V	O_{ax}	O_{eq}	ε (eV)
LUMO+2	$d_{z^2}(V)$	13.5	70.3	10.7	5.5	-2.01
LUMO+3	$d_{xz}(V)-p_x(O_{ax})$	15.6	68.7	9.1	6.6	-1.89
LUMO+1	$d_{xy}(V)-p_x(O_{eq})$	9.4	73.3	2.8	14.5	-2.36
HOMO	π(L)	92.2	2.7	3.2	1.9	-7.82

Table 5

Calculated absorption bands for dioxidovanadium(V) complex.

Wavelength (λ) (nm)	Oscillator strength (*f*)	Orbital distribution	Assignment
417	0.049	HOMO → LUMO (95%)	π(L) → π*(L)
376	0.005	HOMO → LUMO+1 (92%)	π(L) → d_{xy}(V)-p_x(O_{eq})
338	0.072	HOMO → LUMO+3 (68%)	π(L) → d_{xz}(V)-p_x(O_{ax})
289	0.099	HOMO → LUMO+2 (52%)	π(L) → $d_z{}^2$(V)

Table 6

Kinetic parameters (V_{max}, K_M, k_{cat}) for the bromination of phenol red by dioxidovanadium(V) complex.

Catalyst	V_{max} (M min^{-1})	K_M (M)	k_{cat} (h^{-1})
dioxidovanadium(V) complex	5.17×10^{-3}	3.29×10^{-3}	310.20

Graphical Abstract

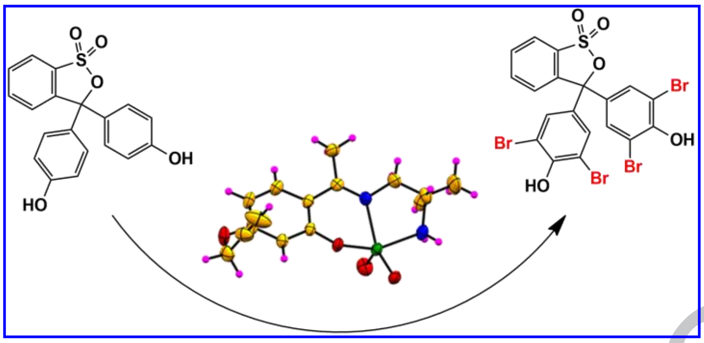

Graphical Abstract

Dioxidovanadium(V) complex was synthesized and structurally characterized. Non covalent interactions in the complex and vanadium dependent bromoperoxidase activity was studied.